

Target isotope effects for vibrationally-resolved electron capture in low-energy collisions of O^{3+} with molecular hydrogen

P. C. Stancil

*Department of Physics and Astronomy and the Center for Simulational Physics,
The University of Georgia, Athens, GA, 30602-2451, USA*

J. G. Wang

*Institute of Applied Physics and Computational Mathematics,
P. O. Box 8009, Beijing 100089, P. R. China*

A. R. Turner

*Department of Chemistry, University of Edinburgh,
West Mains Road, Edinburgh EH9 3JJ, UK*

D. L. Cooper

Department of Chemistry, University of Liverpool, Liverpool L69 7ZD, UK

Abstract

Using a quantum-mechanical molecular-orbital coupled-channel (QMOCC) approach, we investigate single electron capture in collisions of O^{3+} with various molecular hydrogen isotopomers (H_2 , HD, T_2) for collision energies of 1 and 100 eV/u. Potential energy surfaces and nonadiabatic couplings obtained with the spin-coupled valence-bond method are incorporated into QMOCC calculations of vibrationally-resolved cross sections of the product molecular ion. The infinite order sudden approximation is adopted and comparisons of the vibrational distributions are made with the centroid approximation, which incorporates ionization Franck-Condon factors. Intercomparison of the results is used to assess the reliability of the approximations and to give insight into the target isotope effects.

I. INTRODUCTION

Electron capture by ions during collisions with neutral atoms or molecules is an important process in both laboratory and astrophysical plasmas. The ionization and thermal balances of the plasma can be influenced and often dominated by electron capture reactions. Electron capture involving multiply-charged ions can compete with electron-impact excitation in populating excited states of the ion and thereby contributing to the ion emission spectrum.

Electron capture, a process driven by nonadiabatic coupling between different electronic potential surfaces, has been investigated extensively since the 1920s, both experimentally and theoretically. Theoretical studies have, however, focused primarily on collisions of atomic ions with atomic neutrals, and almost exclusively for H and He targets. Collisions with molecular targets, and we focus here primarily on multiply-charged ions, have received considerably less attention due to the increase in the number of degrees of freedom both in the molecular structure and in the scattering calculations. Useful studies of molecular targets involve considering vibrationally-resolved electron capture, thereby significantly increasing the total number of channels in the calculations. The coupling of angular momenta also becomes more elaborate, necessitating the use of various decoupling approximations, so as to make the calculations tractable. The status of theoretical studies of electron capture in collisions of multiply-charged ions with molecular targets has been reviewed by Stancil¹, with emphasis on vibrationally-resolved molecular-orbital coupled-channel (MOCC) techniques relevant to low collision energies (~ 0.1 eV/u to ~ 10 keV/u).

Another aspect in electron capture studies which began to receive attention in the last decade was the influence of target isotope effects. Stancil and Zygelman² predicted that the total electron capture cross section for multiply-charged ion collisions on atomic hydrogen would be significantly suppressed if the target hydrogen was replaced by deuterium. The effect was soon observed in merged-beams measurements³. We have subsequently investigated kinematic isotope effects in a variety of ion-H and ion-He collision systems⁴. The kinematic isotope effect has not been extensively explored for molecular targets. Those studies that are available have considered only molecular hydrogen targets, as summarized briefly in Stancil¹.

In this Discussion article, we extend our vibrationally-resolved QMOCC studies⁵ of $O^{3+} + H_2$ to the molecular hydrogen isotopomers HD and T_2 . HD has been chosen because it is an abundant molecular species in a variety of astrophysical environments, although its small difference in reduced mass relative to H_2 is not expected to result in a significant isotope effect. On the other hand,

the factor of 2.45 increase in reduced mass for T_2 should result in the maximum possible isotope effect in the vibrationally-resolved cross sections for this collision system. We briefly outline the molecular structure of OH_2^{3+} and our scattering approach in Section II. In Section III, the results of the scattering calculations are presented and discussed with comparison to other investigations, while Section IV presents a summary and future directions for this work.

II. MOLECULAR STRUCTURE AND SCATTERING APPROACH

We apply the QMOCC approach using the infinite order sudden approximation (IOSA), as described in Wang *et al.*⁵. The calculations incorporate the electronic adiabatic potentials and nonadiabatic radial couplings computed with the spin-coupled valence-bond (SCVB) method, as described in Turner⁶ and in Wang *et al.*⁵. In addition to the incoming $O^{3+} + H_2$ channel, we consider the two exit channels $O^{2+}(2p3s \ ^3P^o) + H_2^+(X \ ^2\Sigma_g^+)$ and $O^{2+}(2p3s \ ^1P^o) + H_2^+(X \ ^2\Sigma_g^+)$. As rotational couplings are neglected, only states of $^2A'$ symmetry (C_s point group) are included, giving a total of three potential energy surfaces. Jacobian coordinates are adopted, where \mathbf{R} is the internuclear radius vector from the H_2 centre of mass to the oxygen ion, \mathbf{r} is the H-H diatom vibrational stretch vector, and θ is the orientation angle, defined as the angle between \mathbf{r} and \mathbf{R} . Fig. 1(a) shows a slice through the electronic surfaces for $r = 1.4 a_0$ and $\theta = 89^\circ$. The behaviour of the surfaces as a function of r and θ is discussed in Wang *et al.*⁵ but, to summarize, the dependence on θ is weak while significant variation was found when r was varied from 1.2 to 2.0 a_0 . Fig. 1(b) displays the nonadiabatic radial couplings (matrix elements of $\partial/\partial R$) for the same geometries as in Fig. 1(a). Matrix elements of $\partial/\partial r$, which would couple vibrational states within the same electronic manifold, are not considered.

Given the adiabatic potential surfaces and nonadiabatic couplings, a transformation along the R -coordinate is made to a diabatic representation. The resulting electronic diabatic potential curves and couplings are shown in Figs. 1(a) and 1(c), respectively.

In order to perform the scattering calculations, we follow the method of Sidis⁷; our own implementation is outlined in Stancil *et al.*⁸ and in Wang *et al.*⁵. In short, we adopted a perturbed stationary-state (PSS) total system wave function which is expanded over truncated sets of molecular electronic and diatom rotationless vibrational bases. Substitution of this wave function and of the ion-diatom collision system Hamiltonian into the Schrödinger equation gives the PSS scatter-

ing equation in the diabatic representation

$$\begin{aligned} & \{\nabla_R^2 + 2\mu_R[E - \varepsilon_{\gamma v}^d(R, \theta)]\}F_{\gamma v}(R, \theta) \\ & = 2\mu_R \sum_{\gamma' \neq \gamma} \sum_{v'} V_{\gamma v, \gamma' v'}^d F_{\gamma' v'}(R, \theta) \end{aligned} \quad (1)$$

where μ_R is the collision system ion-diatom reduced mass, E is the relative centre-of-mass collision energy, and $F_{\gamma v}(R, \theta)$ is the scattering amplitude for the channel with electronic state γ and vibrational state v . The diabatic vibronic potential coupling is given by

$$V_{\gamma v, \gamma' v'}^d(R, \theta) = \langle \chi_{\gamma v}(r) | V_{\gamma, \gamma'}^d(R, r, \theta) | \chi_{\gamma' v'}(r) \rangle, \quad (2)$$

where the brackets refer to integration over r , $\chi_{\gamma v}(r)$ is the vibrational wave function of the initial or product diatom, $V_{\gamma, \gamma'}^d(R, r, \theta)$ is the electronic diabatic potential coupling, and $\varepsilon_{\gamma v}^d(R, \theta)$ is the diabatic vibronic potential, which we take to be given by

$$\varepsilon_{\gamma v}^d(R, \theta) = \varepsilon_{\gamma}^d(R, r_e, \theta) + \varepsilon_{\gamma v}. \quad (3)$$

$\varepsilon_{\gamma v}$ is the pure, unperturbed vibrational excitation energy of the diatom and $r_e = 1.4 a_0$ for H_2 . Following a partial-wave decomposition, Eqn. (1) is integrated using an implementation of the log-derivative method of Johnson⁹ to obtain S -matrix elements and, ultimately, vibrationally-resolved cross sections at a fixed orientation angle, $\sigma_{\gamma v, \gamma' v'}^{\text{IOSA}}(E, \theta)$. Orientation-averaged cross sections are then given by

$$\begin{aligned} \sigma_{\gamma v, \gamma' v'}^{\text{IOSA}}(E) & = \frac{1}{4\pi} \int_0^{2\pi} d\phi \int_0^{\pi} \sigma_{\gamma v, \gamma' v'}^{\text{IOSA}}(E, \theta) \sin \theta d\theta \\ & = \int_0^{\pi/2} \sigma_{\gamma v, \gamma' v'}^{\text{IOSA}}(E, \theta) \sin \theta d\theta. \end{aligned} \quad (4)$$

Two other approximations are worth considering. The first one, the vibrational sudden approximation (VSA), was introduced in Stancil *et al.*⁸ and is applicable when the diabatic coupling is a weak function of r or the collisional time scale is much shorter than the vibrational period. In the VSA, a Franck-Condon (FC) type approximation is made for the diabatic vibronic coupling of Eqn. (2) giving

$$\langle \chi_{\gamma v}(r) | V_{\gamma, \gamma'}^d(R, r, \theta) | \chi_{\gamma' v'}(r) \rangle \rightarrow V_{\gamma, \gamma'}^d(R, \theta) \langle \chi_{\gamma v}(r) | \chi_{\gamma' v'}(r) \rangle \quad (5)$$

where $\langle \chi_{\gamma v} | \chi_{\gamma' v'} \rangle$ is the square-root of the FC ionization factor for the overlap of the H_2 and H_2^+ vibrational wave functions. The VSA method was tested in Wang *et al.*⁵ and found to give

vibrationally-resolved cross section in fair agreement with the IOSA approach. In another method, the vibrational motion is completely neglected with the scattering calculation performed with only electronic states and electronic couplings. Essentially, the calculations are performed with $r = r_e$, $v = v' = 0$, the FC-like factor in Eq. (5) set to unity, and for one, or a range of, θ -orientations. This approximation, which we refer to as the electronic approximation (EA), has been the dominant approach used within the atomic collision community to study electron capture in ion-molecule collisions. To get an estimate of the vibrationally-resolved cross sections, the centroid approximation (CA) is then applied, which merely involves the multiplication of the resulting EA cross section, $\sigma_{\gamma,\gamma'}^{\text{EA}}$, by a FC factor:

$$\sigma_{\gamma v,\gamma' v'}^{\text{CA}} = \sigma_{\gamma,\gamma'}^{\text{EA}} |\langle \chi_{\gamma v} | \chi_{\gamma' v'} \rangle|^2. \quad (6)$$

In order to compute isotope-dependent cross sections for H₂, HD, and T₂, the reduced mass is adjusted in Eqn. (1), as well as the initial diatom and final diatomic ion vibrational wave functions in Eqn. (2) and the vibrational energies $\epsilon_{\gamma v}$. The required vibrational information is obtained by solving the diatom radial nuclear-motion Schrödinger equation using the Numerov-Cooley method. We adopted the state-of-the-art ground state molecular hydrogen potential described in Jamieson and Zygelman¹⁰ (see also Ref. 11), which includes relativistic, radiative, and isotope-dependent adiabatic corrections. For the molecular ion we used the ground state H₂⁺ potential of Power¹². The computed vibrational binding energies are found to be in excellent agreement with tabulated values. We do not recalculate the nonadiabatic couplings for different isotopes due to the change in the collision system centre of mass, nor are the increases in the electronic ionization potentials of HD or T₂ taken into account. Such effects are expected to be small in comparison to the kinematic-type isotope effects. The increase in the HD and T₂ dissociation energy is taken into account in Eqn. (3).

Following this procedure, we compute the diabatic vibronic potential energies (Eqn. 3) and the vibronic radial couplings (Eqn. 2) for different isotopomers of H₂ for the ground vibrational state $v = 0$ and for the first ten vibrational states, $v' = 0 - 9$, of the H₂⁺ isotopomers for each (r,θ) geometry pair as a function of R . Fig. 2 illustrates the vibronic couplings for the three isotopomers: $(r,\theta) = (1.4 a_0, 89^\circ)$ is shown for the electronic coupling between diabatic states 3 and 2 for various v' . For $v' < 2$, the coupling magnitude decreases with increasing reduced mass. At $v' = 2$, which corresponds to the peak in the ionization FC distributions for both H₂ and HD, their respective couplings are nearly equal, but they are greater than that of T₂. For $v' \gtrsim 4$, the coupling

magnitudes increase with reduced mass, revealing a behaviour opposite to that of the lower ν' couplings. $\nu' = 4$ corresponds to the peak in the T_2 FC distribution. Similar trends are observed for couplings between other electronic states. These coupling behaviours are expected to have a significant influence on the vibrationally-resolved scattering dynamics as will be seen below.

III. RESULTS AND DISCUSSION

We now incorporate the above described diabatic vibronic potentials and couplings into QMOCC-IOSA calculations. In our previous work⁵, we carried out such calculations for the H_2 target from 0.1 to 1000 eV/u. Here we extend that work to considerations of 1 and 100 eV/u collisions of O^{2+} on HD and T_2 . Figs. 3 and 4 display the relative vibrational cross sections ($\sigma_{\gamma\nu,\gamma\nu'}/\sigma_{\gamma,\gamma'}$) for captures into the $^3P^o$ and $^1P^o$ states at 1 and 100 eV/u. Fig. 3(a) shows the results for H_2 and demonstrates that at low collision energies a significant departure is expected from the ionization FC distribution used in the centroid approximation. The QMOCC-IOSA distribution for 1 eV/u peaks at $\nu' = 0 - 1$ and falls-off rapidly for $\nu' > 4$, resulting in a very tight final-state specificity. This is in contrast to an FC distribution, which peaks at $\nu' = 2$ and which has a much broader distribution for larger ν' . As the collision energy is increased to 100 eV/u, however, the QMOCC-IOSA distribution begins to approach the CA result, particularly for $\nu' \geq 2$. The turn-up in the 100 eV/u MOCC-IOSA result for $\nu' = 8$ and 9 is likely to be due to an incomplete H_2^+ vibrational basis.

The situation for HD, shown in Fig. 3(b), is very similar to that for H_2 . This is not unexpected, given that there is only a 33% increase in the collision system reduced mass. However, the QMOCC-IOSA distribution at 1 eV/u is somewhat closer to that of a FC distribution than was the case for H_2 , with the $\nu' < 2$ cross sections being flatter and the $\nu' \geq 5$ cross sections being larger. The 100 eV/u QMOCC-IOSA result for HD is nearly identical to that of H_2 and is seen to approach the FC distribution.

The situation for the most massive isotopomer, T_2 , is considerably different, as shown in Fig. 3(c). Its FC distribution is broader and peaks at $\nu' = 4$. Both the 1 and 100 eV/u QMOCC-IOSA results have maxima which plateau between $\nu' = 2$ and 5, and then decrease for $\nu' < 2$, in a manner reminiscent of the FC distribution. For $\nu' > 5$, the QMOCC-IOSA result for 1 eV/u has a sharp fall-off similar to that seen for the H_2 and HD divergence from the FC distribution. However, at 100 eV/u the QMOCC-IOSA cross sections for $\nu' \geq 4$ are in very good agreement with the FC

distribution. The up-turn for $v' = 8 - 9$ is again likely to be due to an incomplete T_2^+ vibrational basis.

Fig. 4 compares FC distributions (centroid approximation) with the vibrational distributions for capture to the $^1P^o$ state of O^{2+} , obtained from the QMOCC-IOSA calculations. For all vibrational states at 100 eV/u, and for $v' \leq 3$ at 1 eV/u, the distributions are very similar to those shown in Fig. 3 for capture to $O^{2+}(^3P^o)$. However, the distributions at 1 eV/u for $v' > 3$ are quite different, displaying a minimum at $v' = 5, 6,$ and 7 for $H_2, HD,$ and $T_2,$ respectively, with increases for both H_2 and HD for large v' . This is, however, likely to be an artefact of the incomplete vibrational bases, as the diabatic vibronic potential for the $O^{2+}(^3P^o)+H_2^+(v' = 9)$ channel is nearly coincident with the $O^{2+}(^1P^o)+H_2^+(v' = 5)$ channel, and so they have much the same internuclear crossing distance with the entrance $O^{3+}+H_2(v = 0)$ channel. The total capture cross section to $O^{2+}(^3P^o)$ is typically a factor of ~ 5 larger than that for capture to $O^{2+}(^3P^o)$, so that capture probability that would have gone into the $O^{2+}(^3P^o)+H_2^+(v' > 9)$ channels flows instead into the $O^{2+}(^1P^o)+H_2^+(v' = 6 - 9)$ channels, disproportionately. A similar situation occurs for the $O^{2+}(^3P^o)+HD^+(v' = 9)$ and $O^{2+}(^1P^o)+HD^+(v' = 6)$ channels. We would expect that if complete vibrational bases were included in both electronic channels, then the distributions in Figs. 3 and 4 would be more similar. In any event, both figures suggest that as the collision energy and/or the target mass is increased, the vibrational distributions begin to approach the CA result.

The trends in the vibrational distributions that are observed in Figs. 3 and 4 have been noted recently in other calculations, but only three other cases have been studied: $H^+ + H_2$ ($D_2, DT,$ and T_2)¹³, $C^{2+} + H_2$ ¹⁴, and $C^{4+} + H_2$ (D_2 and DT)¹⁵. A number of vibrationally-resolved investigations have been performed for $H^+ + H_2$ and various isotopic combinations, but at such low energies ($\sim 1-20$ eV) that it was unrealistic even to consider trends similar to a FC distribution^{16,17,18,19,20,21,22}. The collision systems which are most similar to that studied here are those for the multiply-charged C^{2+} and C^{4+} ions investigated by Errea *et al.*^{14,15}. They use a similar formalism for the collision dynamics except that the nuclear motion is treated classically: they refer to their approach as the sudden approximation eikonal method. For their study of C^{4+} with $H_2, D_2,$ and $DT,$ Errea *et al.*¹⁵ find that the vibrational distribution departs from a FC distribution at low energies (50 eV/u), but that as the collision energy and/or target mass is increased their computed distributions approach the CA prediction. However, the low-energy behaviour of their vibrational distributions is in marked contrast to those shown in Figs. 3 and 4. They find that as the energy is reduced, the peak in the distribution shifts to larger v' and that the distributions

become broader, with the cross sections for the higher ν' capture channels increasing. This discrepancy is likely to be related to an approximation in their eikonal approach which neglects the energy asymptotics of the vibrational exit channels. That is, the cross section magnitude into a particular vibronic exit channel depends, within the QMOCC-IOSA formalism, on a competition between the location of the diabatic crossing distance, which increases with ν' , and the strength of the vibronic coupling. Both of the $\text{O}^{3+} + \text{H}_2$ and $\text{C}^{4+} + \text{H}_2$ collision systems have fairly large electronic adiabatic avoided-crossing distances, $R > 8.7$ and $8 a_0$, respectively for $r = 1.4 a_0$, so that crossings in the diabatic vibronic channels will increase to larger R with increasing ν' , consequentially resulting in smaller cross sections for increasing ν' . Therefore, we conclude that the sudden approximation eikonal method is unlikely to give reliable predictions of the vibrational distribution for ν' less than the FC peak for low collision energies. This is also suggested by their results for $\text{C}^{2+} + \text{H}_2$, which is the only collision system for which both measurement and calculations have been performed for the vibrational distribution¹⁴. For an experimental collision energy of 580 eV/u, they find that capture to $\text{C}^+(^2\text{S}) + \text{H}_2^+(\nu')$ peaks at $\nu' = 2$, whereas the dominant channel in the experiment is at $\nu' = 0$.

IV. SUMMARY

In this Discussion we have extended our work on vibrationally-resolved electron capture due to collisions of O^{3+} with H_2 to the molecular hydrogen isotopomers HD and T_2 . The calculations have been performed using a fully quantal molecular-orbital coupled-channel (QMOCC) method within the infinite order sudden approximation (IOSA). While the QMOCC-IOSA product molecular ion vibrational distributions are found to be in reasonable agreement with the centroid approximation (CA) at relatively high energies (100 eV/u), significant departures from CA predictions, while not unexpected, were found for low collision energies (1 eV/u). However, it was found that the usefulness of the centroid approximation increased, at all energies, with the increase in the collision system reduced mass. In future work, QMOCC-IOSA calculations will be performed for the other isotopomers (HT, DT, and D_2), more complete product vibrational bases will be included, initial vibrational excited states will be considered, and the computations will be extended over a large range of collision energies from 0.1 eV/u to 1 keV/u.

Finally, one aim of our work has been to incorporate knowledge gained from the study of atom–molecule and singly-charged-ion–molecule collisions²³ in the chemical physics community into

more traditional areas of atomic collisions. However, we are also motivated by observations of X-ray emission from comets for which electron capture from cometary neutrals by highly-charged solar wind ions is the dominant mechanism²⁴. The results of the vibrational distribution trends presented in this Discussion, particularly that found for increasing target mass, suggest the possibility that for studies of > 200 eV/u solar wind ions (e.g., O^{7+}) with cometary molecules (e.g., H_2O , CO , and CO_2), calculations which adopt the centroid or at least the vibrational sudden approximation may be sufficient to provide accurate total and electronic-state-selective cross section data for modeling needs.

Acknowledgments

P. C. S. and J. G. W. acknowledge support from the U.S. National Aeronautics and Space Administration through grant NAG5-11453.

-
- ¹ P. C. Stancil, in *Photonic, Electronic, and Atomic Collisions*, Invited papers of the XXIII International Conference on Photonic, Electronic, and Atomic Collisions, 2003, in press.
 - ² P. C. Stancil and B. Zygelman, *Phys. Rev. Lett.*, 1995, **75**, 1495.
 - ³ M. Pieksma, M. Gargaud, R. McCarroll, and C. C. Havener, *Phys. Rev. A*, **54**, R13.
 - ⁴ D. L. Cooper, N. J. Clarke, P. C. Stancil, and B. Zygelman, 2001, *Adv. Quantum Chem.*, **40**, 37.
 - ⁵ J. G. Wang, P. C. Stancil, A. R. Turner, and D. L. Cooper, 2003, *Phys. Rev. A*, in press.
 - ⁶ A. R. Turner, *Doctoral Thesis*, University of Liverpool, 2002.
 - ⁷ V. Sidis, *Adv. At. Mol. Phys.*, 1989, **26**, 161.
 - ⁸ P. C. Stancil, B. Zygelman, and K. Kirby, in *Photonic, Electronic, and Atomic Collisions*, Invited papers of the XX International Conference on the Physics of Electronic and Atomic Collisions, ed. F. Aumayr, G. Betz, and HP. Winter, World Scientific, Singapore, 1998, p. 537.
 - ⁹ B. R. Johnson, *J. Comput. Phys.*, 1973, **13**, 445.
 - ¹⁰ M. J. Jamieson and B. Zygelman, *Phys. Rev. A*, 2001, **64**, 032703.
 - ¹¹ P. C. Stancil and A. Dalgarno, *Astrophys. J.*, 1997, **490**, 76.
 - ¹² J. D. Power, QCPE Program no. 223, 1973.

- ¹³ D. Elizaga, L. F. Errea, J. D. Gorfinkiel, L. Méndez, A. Macías, A. Riera, and A. Rojas, *J. Phys. B*, 2000, **33**, 2037.
- ¹⁴ L. F. Errea, A. Macías, L. Méndez, I. Rabadán, and A. Riera, *J. Phys. B*, 2000, **33**, L615
- ¹⁵ L. F. Errea, J. D. Gorfinkiel, A. Macías, L. Méndez, and A. Riera, *J. Phys. B*, 1999, **32**, 1705.
- ¹⁶ M. Baer, G. Niedner-Schatteburg, and J. P. Toennies, *J. Chem. Phys.*, 1989, **91**, 4169.
- ¹⁷ A. Ichihara, O. Iwamoto, and K. Yokoyama, *JAERI-Research*, 1998, 98-056.
- ¹⁸ A. Ichihara, O. Iwamoto, and R. K. Janev, *J. Phys. B*, 2000, **33**, 4747.
- ¹⁹ A. Ichihara, O. Iwamoto, and K. Yokoyama, *Atom. Plasma-Mater. Int. Data Fusion*, 2001, **9**, 123.
- ²⁰ P. Krstić, D. R. Schultz, and R. K. Janev, *Phys. Scr.*, 2002, **T96**, 61.
- ²¹ P. Krstić, *Phys. Rev. A*, 2002, **66**, 042717.
- ²² J. G. Wang and P. C. Stancil, *Phys. Scr.*, 2002, **T96**, 76.
- ²³ M. Baer, in *State-Selected and State-to-State Ion-Molecule Reaction Dynamics*, ed. M. Baer and C.-Y. Ng, Wiley, New York, 1992, p. 187.
- ²⁴ T. E. Cravens, *Science*, 2002, **296**, 1042.

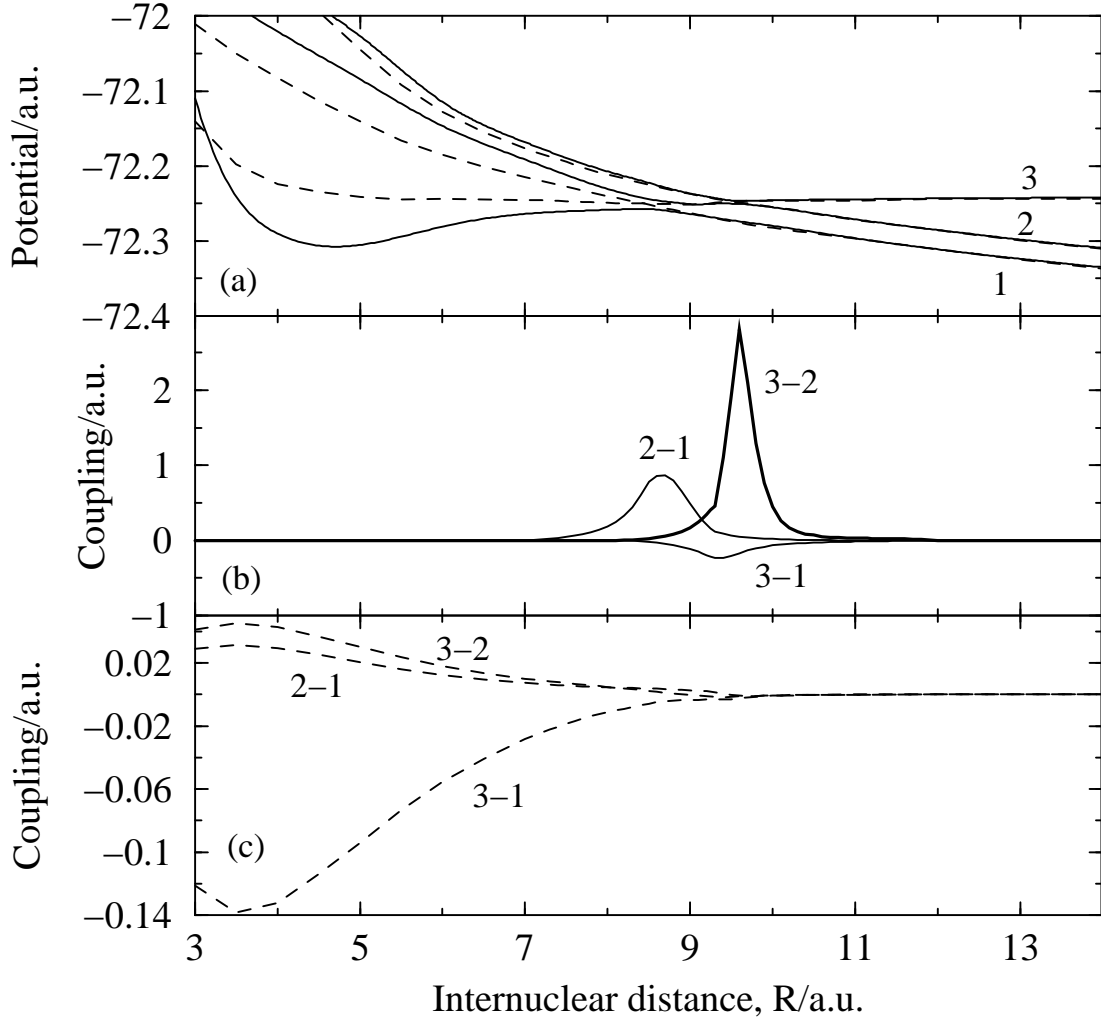


FIG. 1: Electronic potential curves and couplings for OH_2^{3+} as a function of R for $r = 1.4 a_0$ and $\theta = 89^\circ$. (a) Adiabatic and diabatic potentials, (b) nonadiabatic radial couplings, and (c) diabatic couplings. The state labels refer to adiabatic ordering at large R and are: 1 for $\text{O}^{2+}(2p3s \ ^3P^o) + \text{H}_2^+(X \ ^2\Sigma_g^+)$, 2 for $\text{O}^{2+}(2p3s \ ^1P^o) + \text{H}_2^+(X \ ^2\Sigma_g^+)$, and 3 for $\text{O}^{3+}(2p \ ^2P^o) + \text{H}_2(X \ ^1\Sigma_g^+)$.

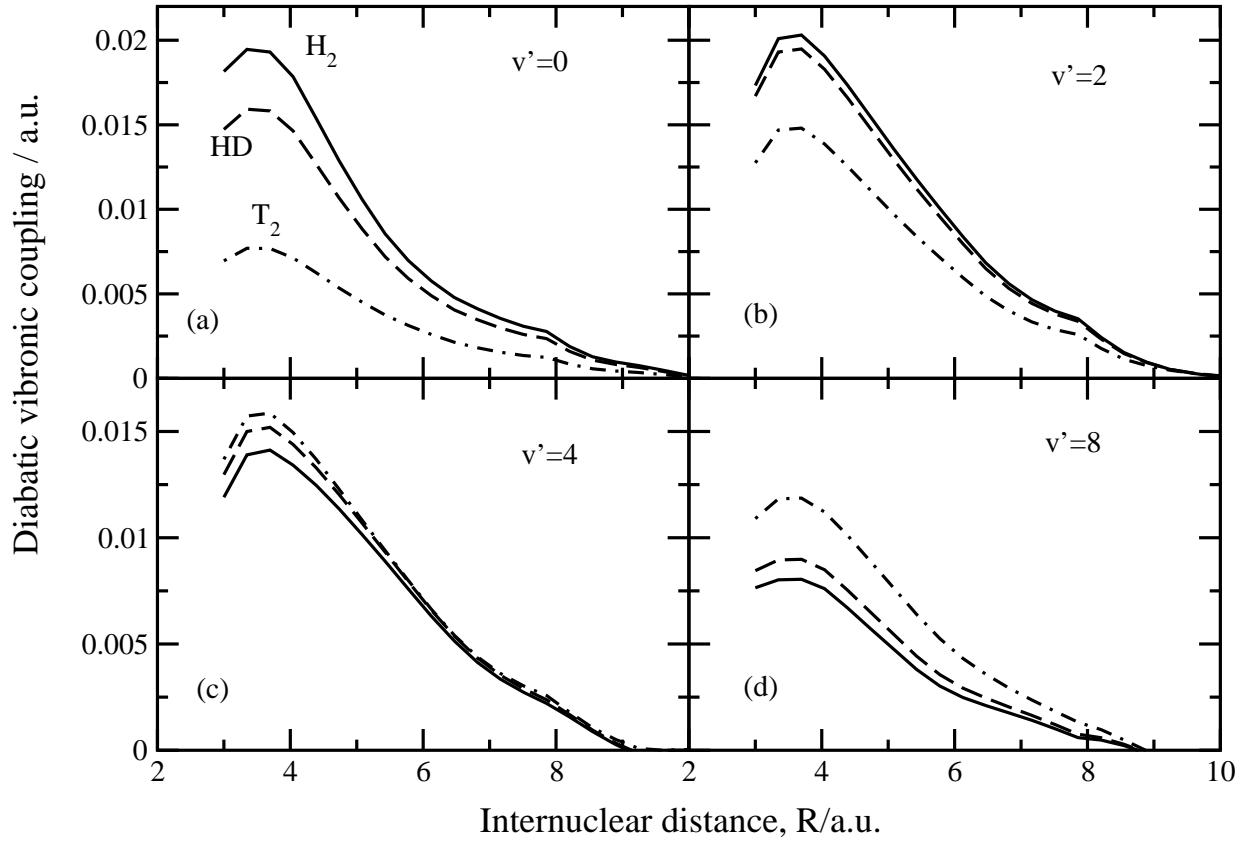


FIG. 2: Diabatic vibronic couplings for 3-2 (capture to $O^{2+}(^1P^o)$) electronic coupling for $\theta = 89^\circ$ with $H_2(v=0)$ [solid lines], $HD(v=0)$ [long dashed lines], and $T_2(v=0)$ [dot dashed lines] and various v' . (a) $v' = 0$, (b) $v' = 2$, (c) $v' = 4$, and (d) $v' = 8$.

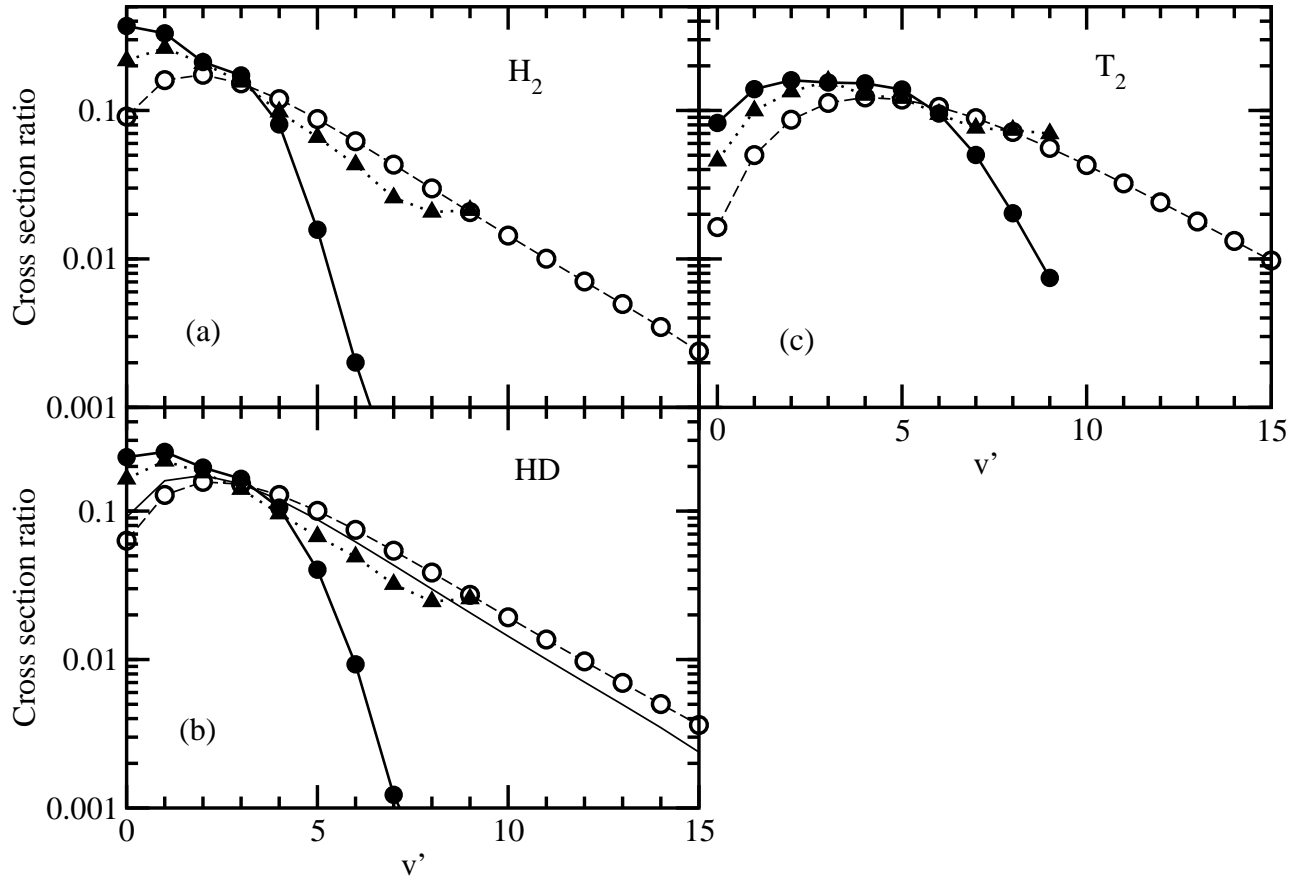


FIG. 3: Product molecular ion vibrational state v' selected electron capture cross section ratio for capture to $O^{2+}(2p3s\ ^3P^o)$ computed with IOSA and compared to the centroid approximation (open circles). (a) $H_2(v=0)$, (b) $HD(v=0)$, and (c) $T_2(v=0)$. QMOCC-IOSA results: 1 eV/u (filled circles) and 100 eV/u (filled triangles).

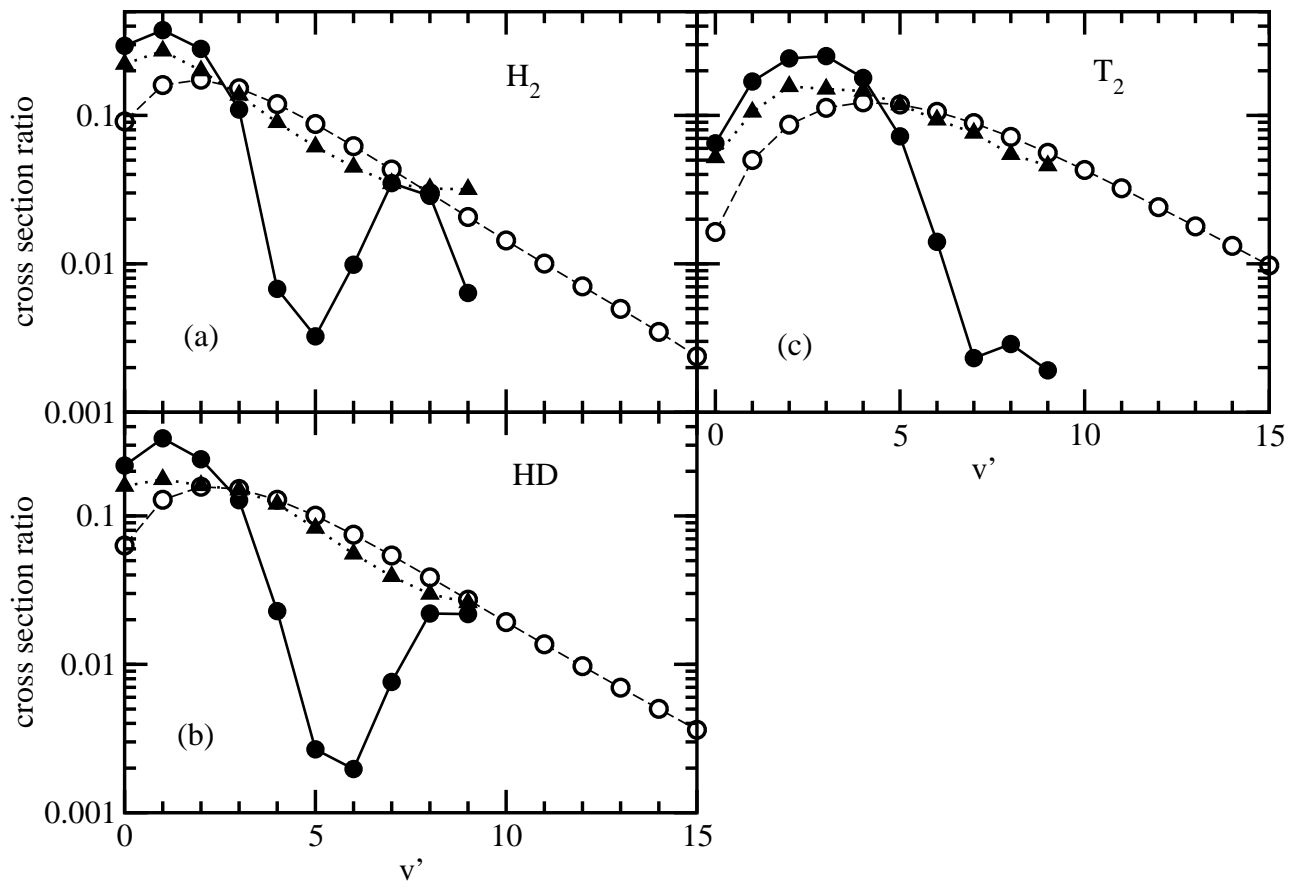


FIG. 4: Same as Fig. 3, but for $O^{2+}(2p3s\ ^1P^o)$.